Galactic population synthesis of radiactive nucleosynthesis ejecta

Sections

1. Introduction
2. Model structure and input parameters
3. Population Synthesis
4. Simulation Results
5. Comparison to data
6. Discussion
7. Summary and outlook

ABSTRACT

Diffuse γ-ray line emission traces freshly produced radioisotopes in the interstellar gas, providing a unique perspective on the entire Galactic cycle of matter from nucleosynthesis in massive stars to their ejection and mixing in the interstellar medium (ISM). We aim at constructing a model of nucleosynthesis ejecta on galactic scale which is specifically tailored to complement the physically most important and empirically accessible features of γ-ray measurements in the MeV range, in particular for decay γ-rays such as ^{26}Al, ^{60}Fe or ^{44}Ti. Based on properties of massive star groups, we developed a Population SYnthesis COde (PSYCO) which can instantiate galaxy models quickly and based on many different parameter configurations, such as the star formation rate (SFR), density profiles, or stellar evolution models. As a result, we obtain model maps of nucleosynthesis ejecta in the Galaxy which incorporate the population synthesis calculations of individual massive star groups. Based on a variety of stellar evolution models, supernova explodabilities, and density distributions, we find that the measured ^{26}Al distribution from INTEGRAL/SPI can be explained by a Galaxy-wide population synthesis model with a SFR of 4–8 $M_\odot\,yr^{-1}$ and a spiral-arm dominated density profile with a scale height of at least 700 pc. Our model requires that most massive stars indeed undergo a supernova (SN) explosion. This corresponds to a SN rate in the Milky Way of 1.8–2.8 per century, with quasi-persistent ^{26}Al and ^{60}Fe masses of 1.2–2.4 $M_\odot$ and 1–6 $M_\odot$, respectively. Comparing the simulated morphologies to SPI data suggests that a frequent merging of superbubbles may take place in the Galaxy, and that an unknown but strong foreground emission at 1.8 MeV could be present.

In this study, we attempt to shift the focus from interpretations of descriptive parameters to astrophysical input parameters to describe the ^{26}Al sky. Modelling an entire Galaxy for

PSYCO

In this paper, we present an alternative approach to modelling the radioactive Galaxy that is specifically adapted to the empirical basis of γ-ray measurements. The essential scientific requirements here are that it can be repeated quickly and in many different parameter configurations and that, at the same time, the astrophysically most important and observationally accessible features can be addressed.

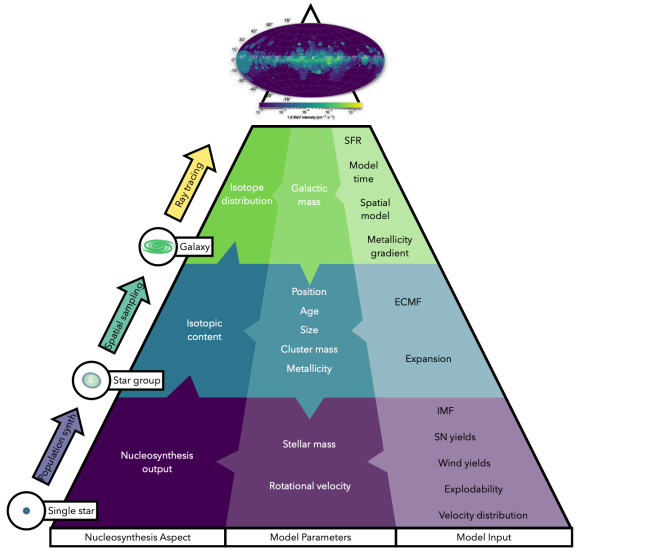

Fig. 1: Structure of the PSYCO model. Using the model input on the right, model parameters are accumulated top-down. The nucleosynthesis aspect on the left is finally built bottom-up to construct all-sky γ-ray maps.

- The production of the nuclear decay radiation in massive stars can be linked with their distribution in the ISM.

- ^{26}Al
  - Half life time 0.7Myr
  - Their study at 1.8 MeV + gamma ray line spectroscopy gave a relation between nucleosynthesis ejecta and the dynamics of massive star groups.
- ^{60}Fe
  - Half life time 2.6Myr
  - Their detection at 1.173MeV and 1.332MeVgave a relation between nucleosynthesis ejecta and the dynamics of massive star groups.

^{26}Al

- Novae
  - $0.2M_{\odot}Myr^{-1}$(Knödlsder)
  - 30%Bennet

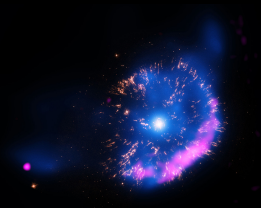

- AGB
  - $0.2M_{\odot}Myr^{-1}$(Knödlsder)

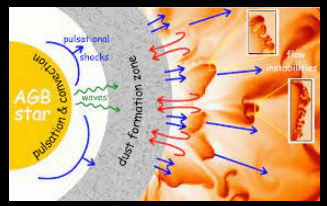

- Massive Star
  - 80% to 90%(Knödlsder)

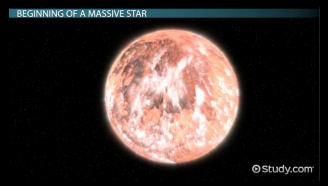

- Cosmic-ray spallation

Model structure and input parameters

- Input=Top down (galactic level to single star properties)
- Nucleosynthesis aspect= bottom-up
- Stellar Mass and time scales
  - SFR as a free parameter
  - Model time is determined by ^{60}Fe=50Myrs
    - Starting empty galaxy gradually filling with stars and radioactive ejecta the evolution gives a CONSTANT STAR FORMATION RATE, leading to a specific gamma ray that can be compared with the data
    - To compare the model with the gamma ray luminosity from the data
- The main physically boundary is in the stellar mass formed in the model
- Mgal=SFR X T_{tot}

Spatial characteristics

- FAST CALCULATION
- ASSUMPTIONS:
  - Position of the observer, gas and stars are CO-ROTATING with respect to the spiral arms therefore we can use a static galactic morphology divided between radial and a vertical component.
  - Distance Sun and center of the galaxy at 8.5kpc (important for than the Luminosity, SFR, mass)
  - Vertical SF density is : $\rho(z; z_0) = z_0^{-1} \exp(-|z|/z_0),$
  - Radial SF density is :

$$\rho(R; R_\mu, \sigma) = \begin{cases} \frac{1}{\sqrt{2\pi}\sigma} \exp\left[-\frac{(R-R_\mu)^2}{2\sigma^2}\right], & \text{if } R \leq 20\,\text{kpc} \\ 0, & \text{else,} \end{cases}$$

    - put together with a 2D structure of 4 logarithmic spirals. Each spiral centroids defined by a rotation angle
  - Around the spiral centroids a Gaussian shaped spread for Star Formation is chosen
    - Spatial distribution of star groups follows the Galactic-wide density distribution

5 galactic morphologies implemented in the model

Central density peak with spriral arms

No Central density peak

Enhanced peak

Pulsars distribution

Exponential radial profile

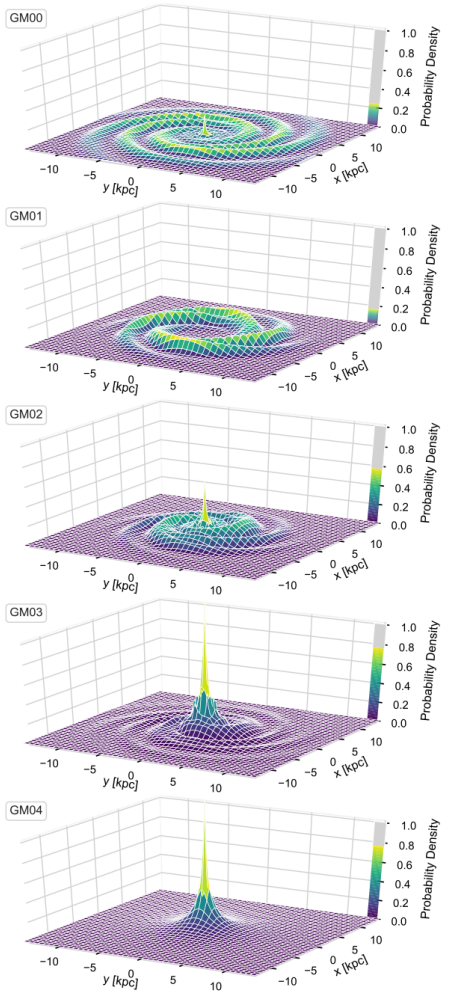

Fig. 2: Radial probability density distributions for star formation. The morphologies GM00–GM04 are ordered from top to bottom by decreasing dominance of the Galactic spiral structure. GM04 is a purely exponential disk.

- Metallicity
  - Decreases with radio
  - It gives the seed nuclei amd the opacity of stellar gas
  - Used in nuclear yields and stellar wind strength
  - Gradient raltive to height

Table 2: Linear parameters for modelling the radial metallicity gradient in the Milky Way according to different heights above the Galactic plane (Cheng et al. 2012). The Intersect is in units of the metallicity, [Fe/H], and the Slope in units of [Fe/H] kpc^{-1}.

Height [kpc]	Slope	Intersect
≥ 1.00	−0.0028	−0.5
0.50–1.00	−0.013	−0.3
0.25–0.50	−0.55	0
0.15–0.25	−0.36	0

Stellar groups

- Distribution function of star forming events
  - Star formation extended or clusters.
  - Assume a single distribution function for all kinds of SF events.
  - In the model we can see it as a probability distribution
  - For events from $5<M_{EC}/M_{o}<10^{7}$:

$$\xi_{\mathrm{EC}}(M_{\mathrm{EC}}) = \frac{dN_{\mathrm{EC}}}{dM_{\mathrm{EC}}} \propto M_{\mathrm{EC}}^{-\alpha_{\mathrm{EC}}},$$

with $\alpha_{\mathrm{EC}} = 2$ in the Milky Way

- Initial mass function

$$\xi_{S55}(M_*) = \frac{dN_*}{dM} = kM_*^{-\alpha}$$

  - Not directly measurable
  - Assumptions, observational uncertainties, and biases
  - They use IMFs from Salpeter, Kroupa and Chabrier
  - Limits: upper limit150M_o and lower limit of 0.012M_o
  - For the upper limit it will vary between each star group.

- Superbubbles
  - Feedbeack in the form of Radiation, thermic and kinetic mechanisms
  - Can be found around each stellar group
  - Size Scale of superbubbles used as spatial modelling of nucleosynthesis ejecta

    CROSSING TIME ----- LIFE TIME OF STELLAR EJECTA. ----- ^{26}Al
  - Radius

$$R_{\text{bubble}}(t) = xL_{\text{W}}^{1/5}t^{3/5} \qquad x = \alpha\rho_0^{-1/5}.$$

  - $L_w=10^{38}$ergs/s, $x=4 \times 10^{3}kg^{-1/5}m^{3/5}$
  - Every cluster gets a psotion according to the galactic morphology, the position gives its matalicity

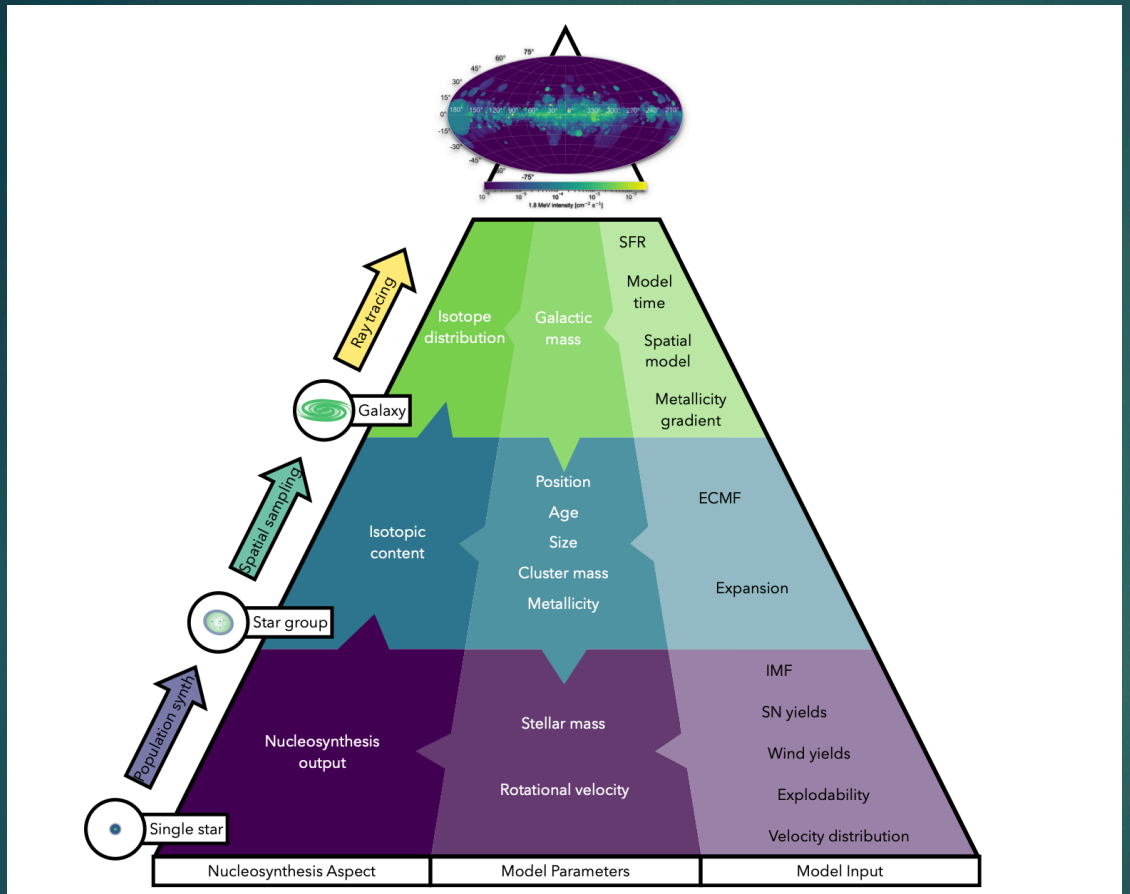

Fig. 1: Structure of the PSYCO model. Using the model input on the right, model parameters are accumulated top-down. The nucleosynthesis aspect on the left is finally built bottom-up to construct all-sky γ-ray maps.

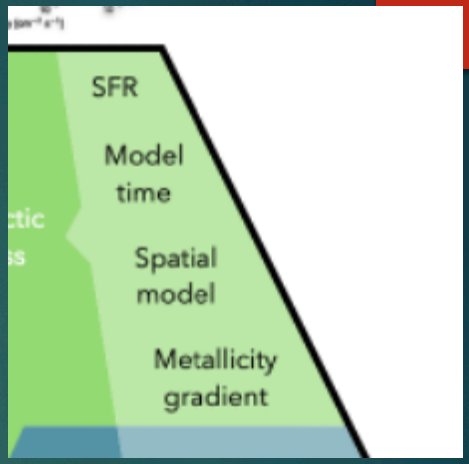

Stellar parameters

- Stellar rotation
  - advection
  - Turbulent diffusion
  - Enhances convective regions inside the star
  - Stellar winds occur earlier
  - Wind phase and lifetime increases

- Stellar rotation implementation
  - Randomly sampling a rotational velocity for each forming star
  - Using Glebocki stellar rotation properties for each spectral class
  - Rotational velocities are weighted with the average inclination angle of stars
  - Rotation velocities are fitted for each spectral class by a Gaussian

- Explodability
  - If after the stellar collapse there is an explosion or not
  - Processed material is ejected in the SNe
  - The ratio of $^{60}Fe/^{26}Al$ is an important tracer of explodability effects on chemical enrichment

- Different simulations
- Wind ejecta remains unaffected by explodability

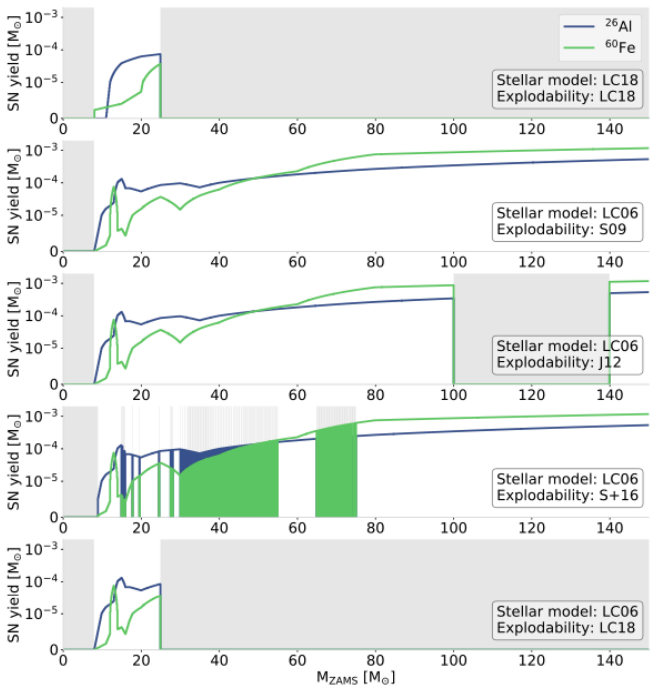

Fig. 3: ^{26}Al (*blue*) and ^{60}Fe (*green*) yields from SNe by Limongi & Chieffi (2006) for different explodability models. Stars with an initial mass inside the grey shaded regions eject no material during the SN. Islands of explodability following each other closely appear as green regions.

- Nucleosynthesis yields
  - Total mass produced by each star over its life time
  - Depending on rotation, mixing, eind,metallicity and nuclear physics
  - Different models as we can see from the figure
  - The model used are Limongi & Chieffi 2018 and Limongi & Chieffo 2006
    - production and ejection in time- resolved evolutionary tracks over the entire lifetime of the stars therefore less extrapolations

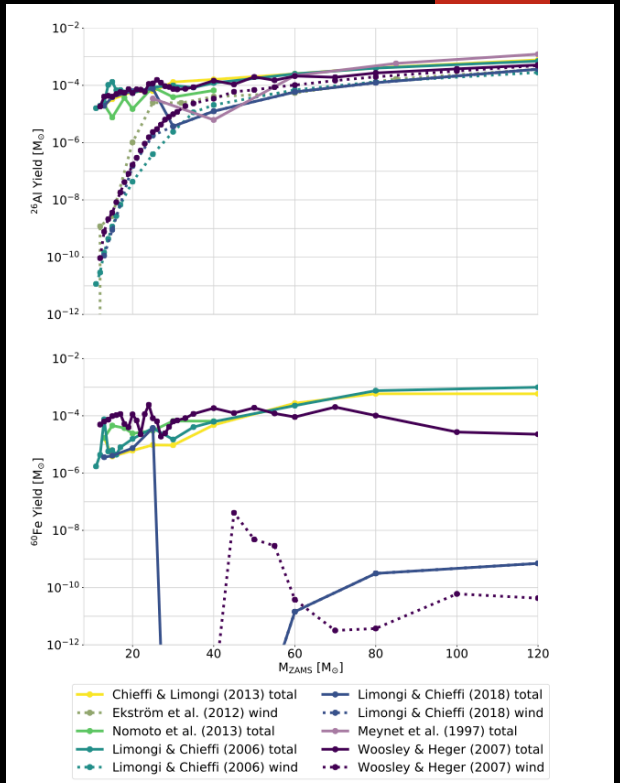

Fig. 4: Nucleosynthesis yields (top ^{26}Al, bottom ^{60}Fe) for a selection of stellar evolution models, separated into the stellar wind and total contribution (wind + SN).

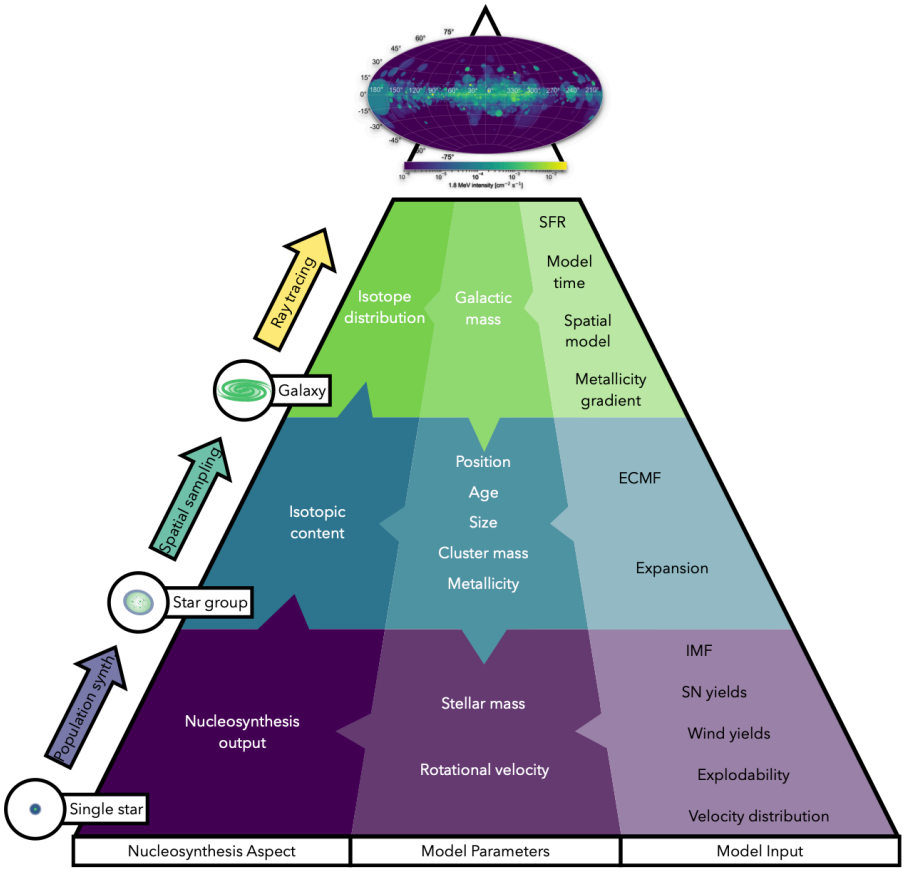

Fig. 1: Structure of the PSYCO model. Using the model input on the right, model parameters are accumulated top-down. The nucleosynthesis aspect on the left is finally built bottom-up to construct all-sky γ-ray maps.

- Stellar binaries
  - Unknown influence of of many stellar evolution parameters
  - Binary Yields calculations by Brinkman are used in PSYCO, to see how they change
  - The fact that a star has or not a companion was sampled randomly
  - SN ejecta was added
  - Results:
    - ^{26}Al
      - Binary wind is not so important after 10Myr
      - Reduction of it after 15Myr, due to the reduction of wind yield in primary stars of 25 to 30M_o
      - After 17Myr there is an increase in binary wind yield

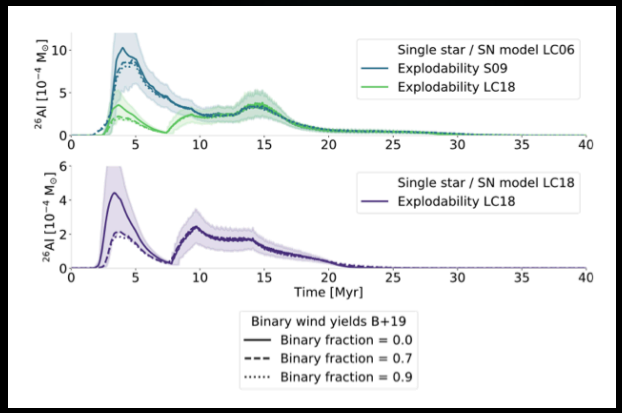

Population synthesis

- Relates the integrated signal of a composite system with the evolutionary properties of its constituents

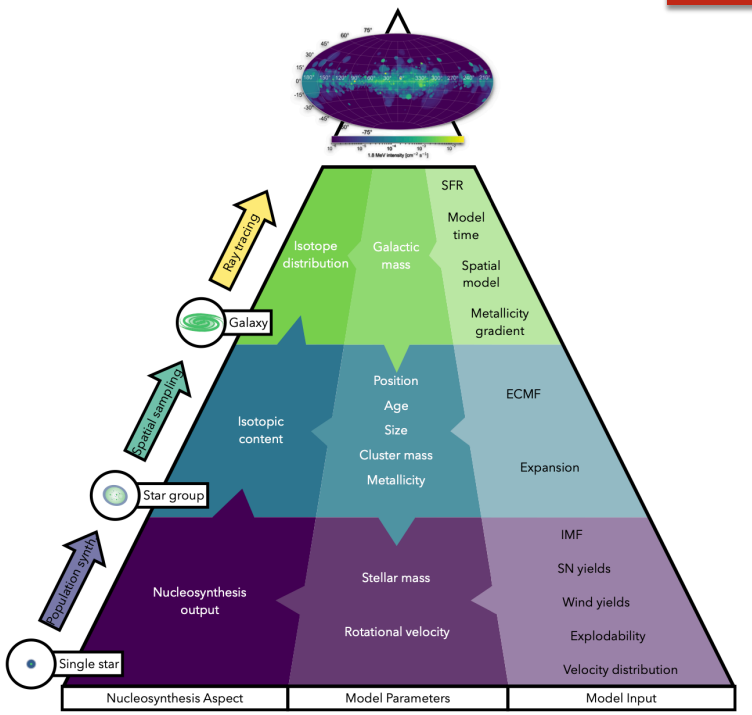

Fig. 1: Structure of the PSYCO model. Using the model input on the right, model parameters are accumulated top-down. The nucleosynthesis aspect on the left is finally built bottom-up to construct all-sky γ-ray maps.

- STAR GROUP
  - Where the time profile of the stars properties are integrated over the entire mass range, weighted with the initial mass function

$$\Psi(t) = A \int_{M_{*,\min}}^{M_{*,\max}} \psi(M_*, t)\, \xi(M_*)\, dM_*$$

  - Problems with IMF, that by integrating the bias grows, they decided to use a discrete population synthesis by Monte Carlo sampling.
  - STEPS TO OBTAIN THE CUMULATIVE PROPERTIES:

1. use optimal sampling technique to shape the IMF

   Total mass M_{EC} to be conserved
2. Stellar rotation assigned to each star according to their spectral class(why the gaussian)
3. Assigning of position srawn from the Galactic density distribution and metallicity

- The tracks of LC2006 AND LC2018 are only for some solar masses
  - SOLUTION
    - GRID of stellar masses in 0.1M_o steps and times in 0.01Myr
    - Interpolation, and extrapolation for stellar masses above 120M_o and below 13M_o

Effects of the main physical input parameters

- 10^4 M_o Cluster
- Models od LC 2018
- LC2006 for explodability
- IMF:
  - Amplitude
  - S55 problem it is unbroken for low mass stars
- Metallicity:
  - Less metal in the original forming gas
  - Iron produced quickly, small amount to C or He shell
  - Decrease of opacity decrease in ^{26}Al
- Explodability
  - Only way ^{60}Fe is ejected
- Rotation
  - Core pressure reduce lifetime extended

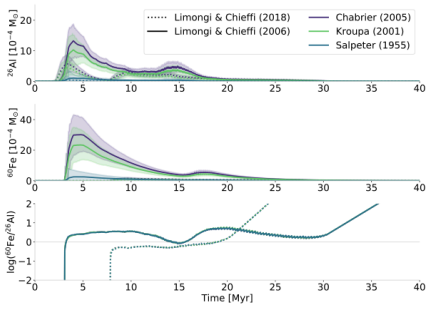

(a) Variations with different IMFs.

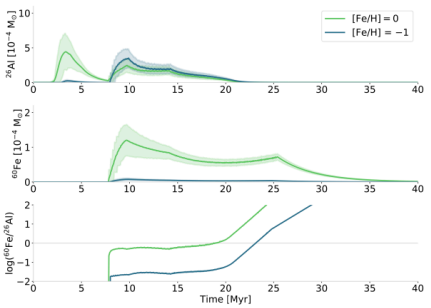

(b) Variations with different metallicities.

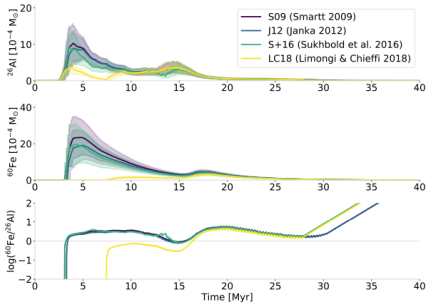

(c) Variations with different explodabilities.

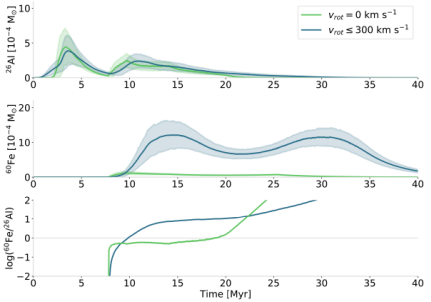

(d) Difference when including rotation.

MASS RATIO

- Crucial information for stellar physics

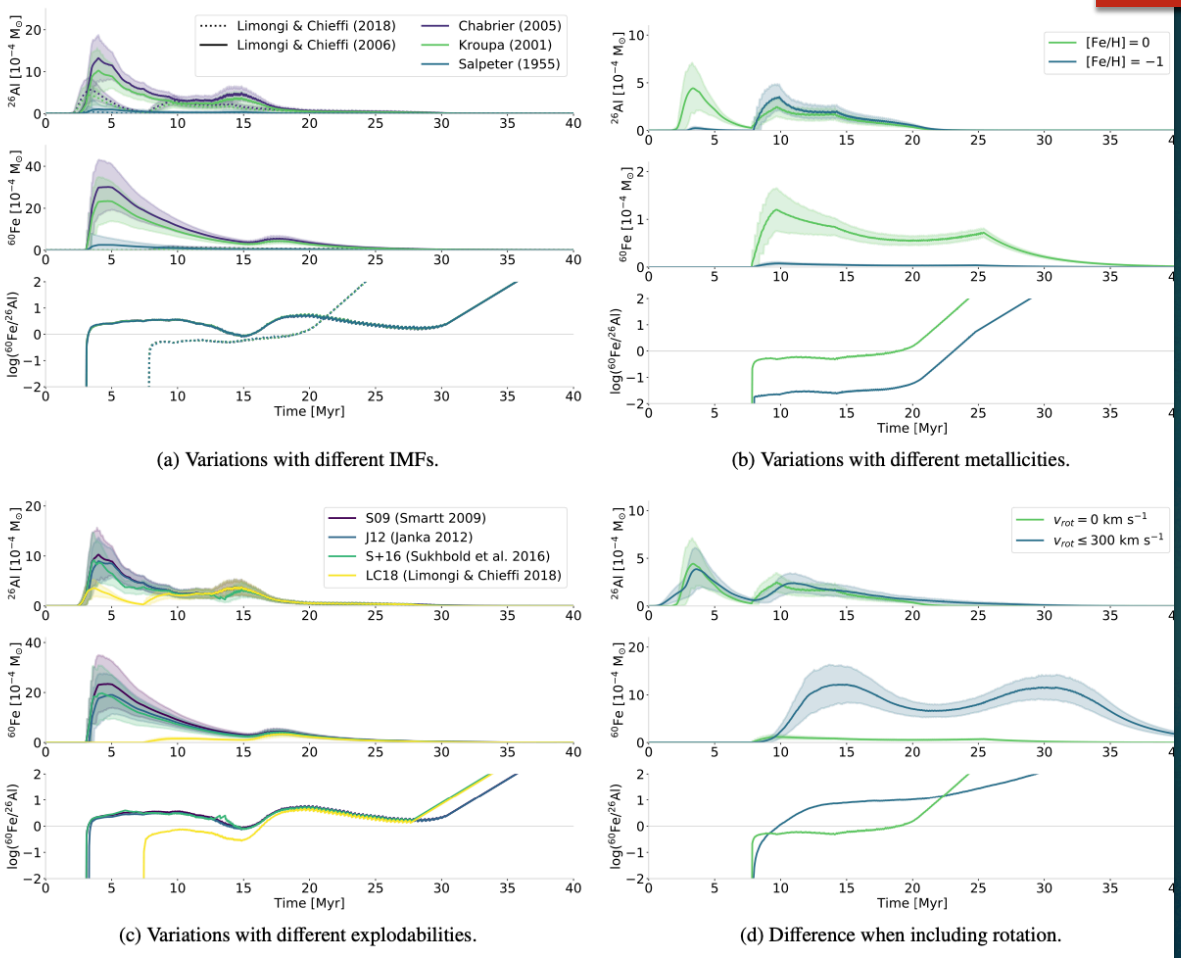

- Galaxy
  - Calculate a total galactic mass that is processed into stars with a constant SFR over 50Myr
  - Embedded Cluster mass function similar to IMF
  - Mass, time and spatial dimension
  - Star groups information changed from 3D to 2D by line of sight integration. This way it can be confronted with gamma ray measurements
    - Creating a spatial gamma-ray emission model

$$L_{n,\odot} = \frac{L_n}{M_\odot} = \frac{p_{E_\gamma}}{M_{m,\mathrm{u}}\tau_n},$$

EVALUATION OF PSYCO MODELS

We have evaluated a grid of models, varying our input parameters with SFR $\in \{2, 4, 8\}\,M_\odot\ yr^{-1}$, scale height $z_0 \in \{0.1, 0.2, 0.3, 0.5, 0.7\}$ kpc, density profiles GM00–GM04, the two stellar evolution models LC06 and LC18, and the explodabilities S09, and S+16 (and LC18 to match the LC18 stellar evolution model). We chose to use only the IMF K01. For each parameter value combination, 100 MC runs are performed to estimate stochastic variations, which in total amounts to 30000 simulated PSYCO maps.

- OBJECTIVE
  - Correlation between parameters and put an uncertainty to those

SIMULATION RESULTS

to those. Naturally, the SFR and explodability have an impact on the total amount of ^{26}Al and ^{60}Fe present in Galaxy: For LC18 (stellar evolution model and explodability), the total galactic ^{26}Al mass follows roughly a linear trend $M_{26}/M_\odot \approx 0.25 \times \mathrm{SFR}/(\mathrm{M}_\odot\,\mathrm{yr}^{-1})$; for other explodabilities, the SFR impact is larger $M_{26}/M_\odot \approx 0.31$–$0.52 \times \mathrm{SFR}/(\mathrm{M}_\odot\,\mathrm{yr}^{-1})$. For ^{60}Fe, the effects of explodability are reversed since ^{60}Fe is only ejected in SNe. We find $M_{60}/M_\odot \approx 1.72 \times \mathrm{SFR}/(\mathrm{M}_\odot\,\mathrm{yr}^{-1})$ for LC18, and $M_{60}/M_\odot \approx 0.28$–$1.27 \times \mathrm{SFR}/(\mathrm{M}_\odot\,\mathrm{yr}^{-1})$ for the other explodability models. The resulting mass ratio ^{60}Fe/^{26}Al has therefore almost no SFR-dependence, and we find ^{60}Fe/^{26}Al of 0.9 for LC18, up to 7.1 for LC06. We note that there are crucial differences in the flux, mass, and isotopic ^{60}Fe/^{26}Al ratio: Given that the γ-ray flux F_n of an radioactive isotope n is proportional to $M_n p_{\gamma,n} m_n^{-1} \tau_n^{-1}$ (see Eq. (9)), the flux ratio of ^{60}Fe to ^{26}Al in the Galaxy as a whole is

$$\frac{F_{60}}{F_{26}} = \frac{p_{60}}{p_{26}} \cdot \frac{\tau_{26}}{\tau_{60}} \cdot \frac{m_{26}}{m_{60}} \cdot \frac{M_{60}}{M_{26}} = 1.00 \cdot 0.27 \cdot 0.43 \cdot \frac{M_{60}}{M_{26}} = 0.12 \frac{M_{60}}{M_{26}}.$$

The SN rates (SNRs) from these model configurations are directly proportional to the SFR, as expected, and follow the trend

$\mathrm{SNR/century}^{-1} \approx 0.37$–$0.56 \times \mathrm{SFR}/(\mathrm{M}_\odot\,\mathrm{yr}^{-1})$, with the explodability LC18 giving the lowest SNR and S09 the highest. The values above are independent of the chosen density profiles. By contrast, the 1.809 MeV (^{26}Al) and 1.173 and 1.332 MeV (^{60}Fe) fluxes are largely dependent on the chosen spiral-arm promi-

Overall Apperance

- Convergence of the model after 50Myr
- SFR change chenges only the amplitude
- Evaluation of the models at 50Myr

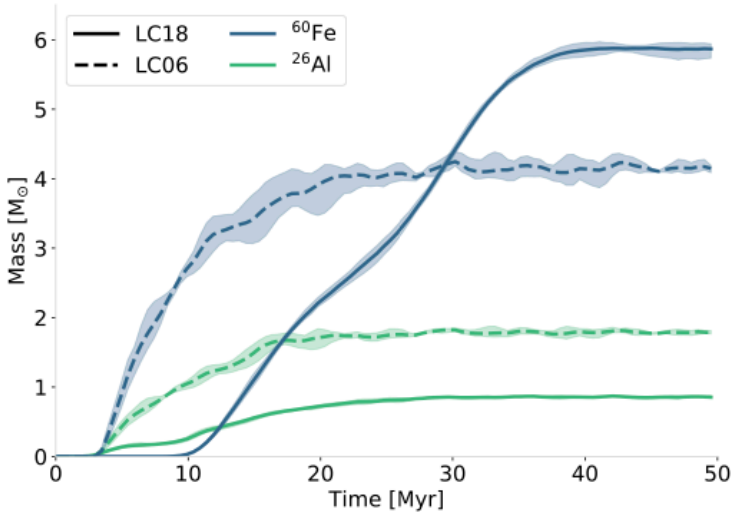

Fig. 7: Steady-state settling time of the total ^{60}Fe (*blue*) and ^{26}Al (*green*) in PSYCO galaxy models. Shaded regions denote the 68th percentile of 100 MC model runs. All models are based on evolutionary tracks LC06 (dashed lines) or LC18 (solid lines) and explodability models S09 and LC18, respectively, for SFR = 4 $M_\odot$ yr^{-1} and the K01 IMF.

- GM03: 50% of the total ^{26}Al gamma ray flux is received within 6 kpc
- Remember Local arm 2kpc, 30% enclosed
- Flux received excludes galactic center
- 0.3% of all cases 90% of the total flux comes from 6kpc
- Local components outweigh Galactic emission
- Comparing to other simulations like the one of Rodgers-Lee best agreement with GM03

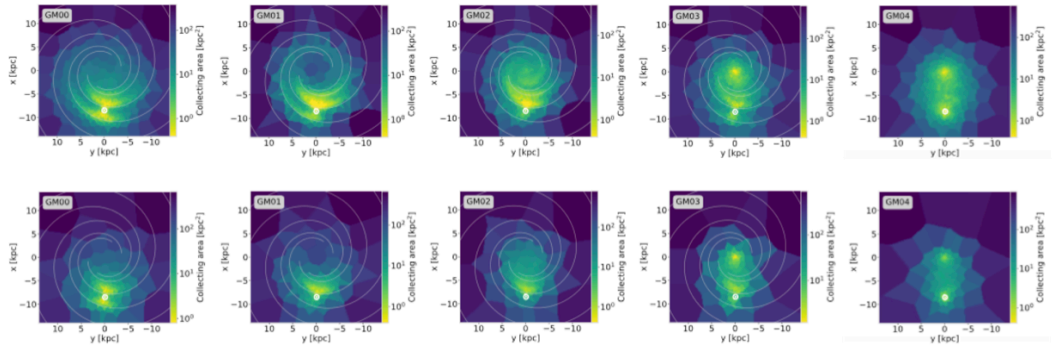

Fig. 8: Radial distribution of modelled flux contributions for a theoretical observer (white circle) from ^{26}Al (*top*) and ^{60}Fe (*bottom*) decay. Each column represents average results of 500 model instantiations based on the density profiles GM00–GM04 (grey boxes). The models shown are stellar evolution models LC06, explodability S09, IMF K01, and SFR = $M_\odot\,\mathrm{yr}^{-1}$. The latter corresponds to a total mass of $1.8 \pm 0.2\,\mathrm{M}_\odot$ and $4.2 \pm 0.2\,\mathrm{M}_\odot$ of ^{26}Al and ^{60}Fe, respectively. Adaptive spatial binning (Cappellari & Copin 2003)is used to obtain Voronoi tessellations as spatial bins, each of which contribute a flux of $10^{-6}\,\mathrm{ph\,cm^{-2}\,s^{-1}}$ for the observer. The colour scale refers to the collecting area covered by each such pixel.

Comparisson to data

- Galactic ^{26}Al and ^{60}Fe fluxes for gamma ray signals
  - Total flux and flux distribution
    - Measurements almost independent in morphology
    - Absolute measurements are important for thr model constraints

5 %), so that the absolute measurements of $F_{26} = (1.71 \pm 0.06) \times 10^{-3}$ ph cm^{-2} s^{-1} (Pleintinger et al. 2019) and $F_{60} = (0.31 \pm 0.06) \times 10^{-3}$ ph cm^{-2} s^{-1} (Wang et al. 2020a) are impor-

    - Density profiles important
    - GM03 lowest flux and GM01 highest
    - Inner Galaxy used for comparisson. Surface brightness high
    - Scale height for the density profile(galaxy size)
      - Smaller scale heights = larger fluxes
      - Stronger for ^{60}Fe
        - Fills older and larger bubbles
      - Density profiles closer to the observer

- Radial distribution and flux
  - Bright regions where most of the flux originates
  - local flux contributions + spiral arms shape the resulting images
  - GM03 AND GM04 a central flux + local contribution = expected profile for classical novae. COMPTEL nor SPI map have not seen the central flux

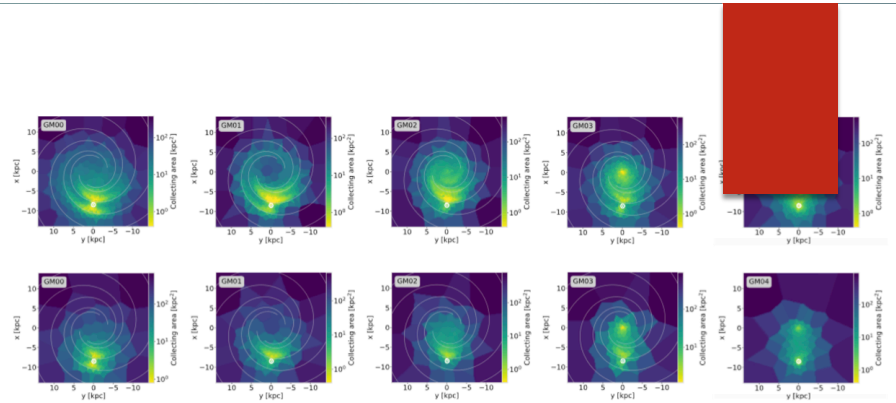

Fig. 8: Radial distribution of modelled flux contributions for a theoretical observer (white circle) from ^{26}Al (*top*) and ^{60}Fe (*bottom*) decay. Each column represents average results of 500 model instantiations based on the density profiles GM00–GM04 (grey boxes). The models shown are stellar evolution models LC06, explodability S09, IMF K01, and SFR = $M_\odot\,\mathrm{yr}^{-1}$. The latter corresponds to a total mass of $1.8 \pm 0.2\,\mathrm{M}_\odot$ and $4.2 \pm 0.2\,\mathrm{M}_\odot$ of ^{26}Al and ^{60}Fe, respectively. Adaptive spatial binning (Cappellari & Copin 2003)is used to obtain Voronoi tessellations as spatial bins, each of which contribute a flux of 10^{-6} ph cm^{-2} s^{-1} for the observer. The colour scale refers to the collecting area covered by each such pixel.

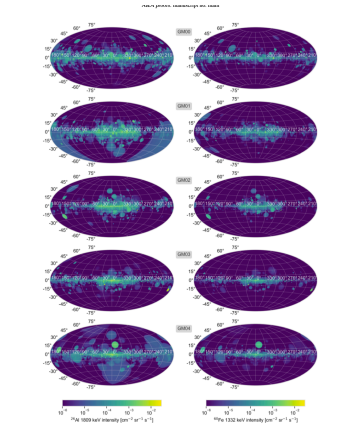

Fig. 9: Simulated full-sky γ-ray maps of the 1.8 MeV line from ^{26}Al decay (*left*) and the 1.3 MeV line from ^{60}Fe decay (*right*) constructed with PSYCO. Each row represents an individual MC run based on a different density profile (gray boxes) with a scale height of 300 pc. Nucleosynthesis yields are based on LC06 with the S09 explodability and the K01 IMF.

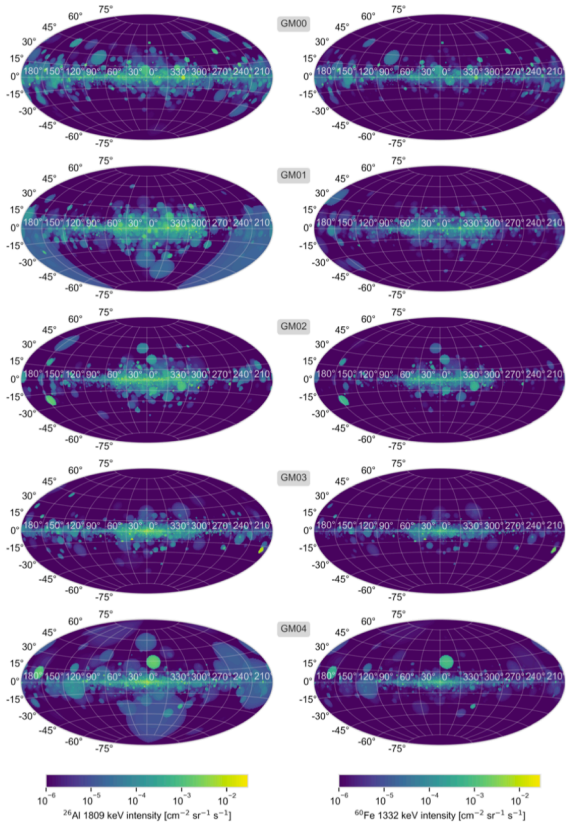

Fig. 9: Simulated full-sky γ-ray maps of the 1.8 MeV line from ^{26}Al decay (*left*) and the 1.3 MeV line from ^{60}Fe decay (*right*) constructed with PSYCO. Each row represents an individual MC run based on a different density profile (gray boxes) with a scale height of 300 pc. Nucleosynthesis yields are based on LC06 with the S09 explodability and the K01 IMF.

- Likelihood comparisson
  - Comparisson of individual models in image space not the best approach due to the stochastic approachof PSYCO and the data set projected back to the celestial sphere
  - Solution: go to the instruments natove dataspace
  - Image convolved with the image response functions
  - Used the all sky maps of COMPTEL and SPI
  - Keep in mind that PSYCO cannot map individual morphological features of the Milky Way

$$\mathrm{TS} = 2(\log(\mathscr{L}(D|M_0)) - \log(\mathscr{L}(D|M_1))),$$

- M1= image + background
- Mo=instrumental background model
- Null – alternative
- Probability of it occurring by chance

- Test statistic relative measure of the fit quality
- GM 00 best cases and GM04 typically used model
- SFR no morphological impact
- TS of exponential profiles had a central peak that data has not
- Notice GM00:
  - Best TS values
  - The only model to increase with height as well and SFR.
  - Height gives the SPI data of high latitudes contributions.

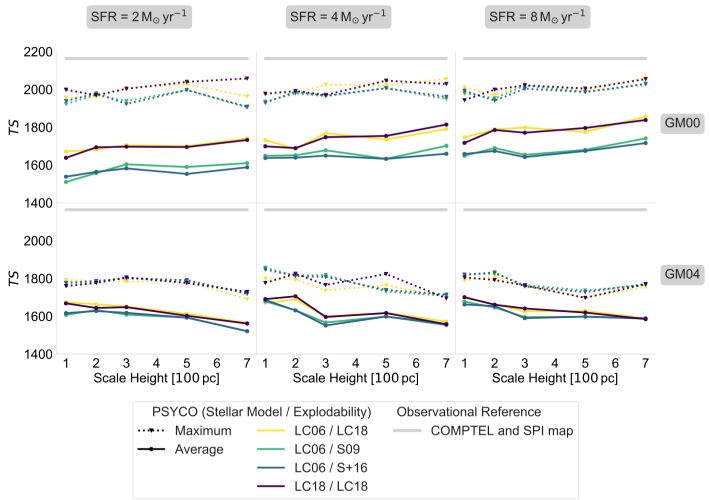

Fig. 10: Likelihood ratio of 6000 sky maps modelled with PSYCO relative to the likelihood of a background-only fit with the SPI. Dots and solid lines denote the average values from 100 MC runs as a function of scale height. The colours correspond to stellar model configuration as noted in the legend. Triangles mark the maximum TS value obtained from the 100 MC samples for each model configuration. The thick gray lines denote the reference value obtained with COMPTEL (TS = 2160) and SPI (TS = 2166).

BEST MODEL

- Peak towards the inner galaxy and the galactic anticenter
- Spiral arms gaps
- Homogenous
- Problem the resolution of COMPTEL and SPI are of 3° and a sensitivity worse than the model

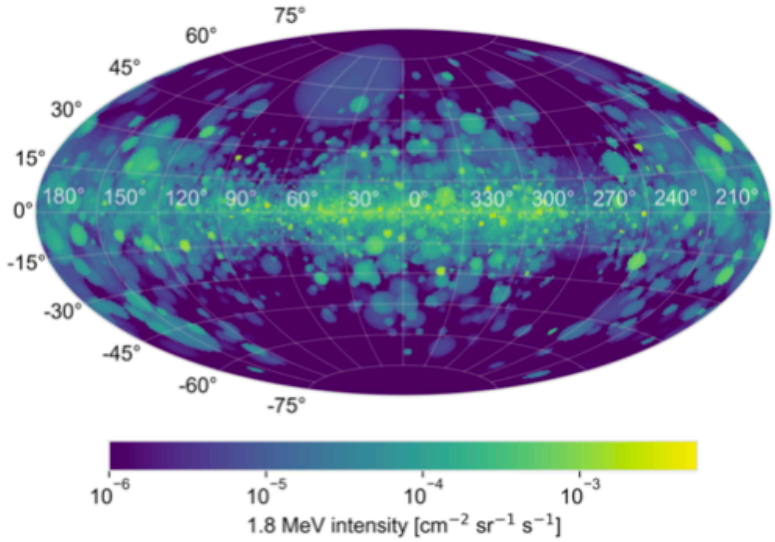

Fig. 11: Best fitting sky map with TS = 2061 out of 30000 PSYCO models. It is based on GM00 with 700 pc scale height, SFR = 8 $M_\odot$ yr^{-1}, IMF K01, stellar models LC06, and explodability LC18.

- Solution:
  - Convolve it with a 2D Gaussinan of 2°
  - Minimum intensity of 5 x 10^{-5} ph s^{-1} cm^{-2} sr^{-1}

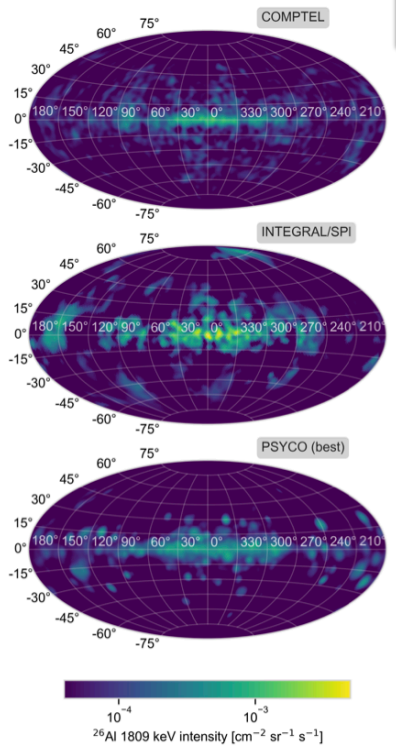

Fig. 12: Compilation of observational maps (top: COMPTEL; middle: SPI) compared to our best-fitting PSYCO simulation, adopted to match the instrument resolution of 3°. The minimum intensity in the maps is set to 5×10^{-5} ph s^{-1} cm^{-2} sr^{-1} to mimic potentially observable structures.

DISCUSSION

- DEGENERACY between superbubbles physics, yiels and star formation
  - The ejecta simulation gives a round shape around the star in reality this is not the case. Even the hypothesis of homogeneaty it's not always verified.
- Star Formation and Supernova rate
  - Using the fluxes from SPI and we get a SNR of about 1.8-2.8 per century
  - Statistical uncertainties of 2-4%
  - Total mass of Al=1.2-2.4M_o
  - Total mass of Fe=1-6M_o
- $^{60}Fe/^{26}Al$ ratio
  - Depend on the stellar evolution and explodability
  - Due to the fact that the measured value of Al is higher than the one of PSYCHO, the flux ratios are higher than the measured one.
  - Difficult to meausure Fe lines in SPI due to the increasing background of Co, the uncertainties could grow to 0.4
  - The Al anf Fe distributons go accordingly with what expected, Al produces in radius from 2.8 to 6kpc. And Fe produced up to 4 kpc.
  - Improvement of the model for the Al flux(increase it)
    - Additional strong local component at high latitudes, or a particularly enhances Local Arm towards to the Galactic anticenter

- Foreground emition and superbubble merging
  - Once more we can talk about the problem with Al
    - Understimation on the bubble size and on the gamma emission
      - SFR near the Solar System larger than what expected and more clustered
      - Clustered SF releases energy more concentrated

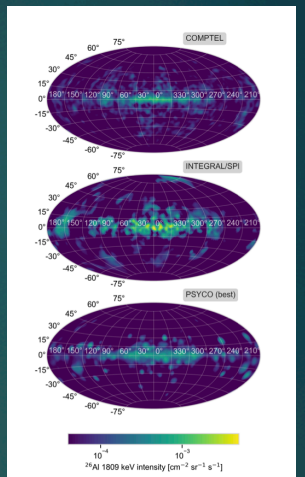

Fig. 12: Compilation of observational maps (top: COMPTEL; middle: SPI) compared to our best-fitting PSYCO simulation, adopted to match the instrument resolution of 3°. The minimum intensity in the maps is set to 5×10^{-5} ph s^{-1} cm^{-2} sr^{-1} to mimic potentially observable structures.

SUMMARY AND OUTLOOK

- Works for the major feautures of the observed sky
- Fails to reproduce the all sky gamma ray flux
- Mismatches at higher latitudes
- Include Cygnus OB2, Scorpius Centau- rus or Orion OB1 associations
  - Spherical volume approximarion Inadequate
- Weaker structure predictions identification:
  - Use COSI data for the Fe, this will give a better sensitivity after two years. There is SMEX mission for 2026 that will get the data.
  - Use the data that is being collected by INTEGRAL until 2029